OncoTargets and Therapy

Dovepress
open access to scientific and medical research

Open Access Full Text Article

ORIGINAL RESEARCH

MIR22HG As A Tumor Suppressive lncRNA In HCC: A Comprehensive Analysis Integrating RT-qPCR, mRNA-Seq, And Microarrays

This article was published in the following Dove Press journal:
OncoTargets and Therapy

Li Gao,[1,*] Dan-dan Xiong,[1,*] Rong-quan He,[2] Xia Yang,[1] Ze-feng Lai,[3] Li-min Liu,[3] Zhi-guang Huang,[1] Hua-yu Wu,[4] Li-hua Yang,[2] Jie Ma,[2] Sheng-hua Li,[5] Peng Lin,[6] Hong Yang,[6] Dian-zhong Luo,[1] Yi-wu Dang,[1,*] Gang Chen[1,*]

[1]Department of Pathology, First Affiliated Hospital of Guangxi Medical University, Nanning, Guangxi, Zhuang Autonomous Region 530021, People's Republic of China; [2]Department of Medical Oncology, First Affiliated Hospital of Guangxi Medical University, Nanning, Guangxi, Zhuang Autonomous Region 530021, People's Republic of China; [3]School of Pharmacy, Guangxi Medical University, Nanning, Guangxi, Zhuang Autonomous Region 530021, People's Republic of China; [4]Department of Cell Biology and Genetics, School of Pre-Clinical Medicine, Guangxi Medical University, Nanning, Guangxi, Zhuang Autonomous Region 530021, People's Republic of China; [5]Department of Urology Surgery, First Affiliated Hospital of Guangxi Medical University, Nanning, Guangxi, Zhuang Autonomous Region 530021, People's Republic of China; [6]Department of Ultrasound, First Affiliated Hospital of Guangxi Medical University, Nanning, Guangxi, Zhuang Autonomous Region 530021, People's Republic of China

*These authors contributed equally to this work

Correspondence: Gang Chen
Department of Pathology, First Affiliated Hospital of Guangxi Medical University, 6 Shuangyong Road, Nanning, Guangxi 530021, People's Republic of China
Tel +0086-771-5356534
Fax +86 0771-5356534
Email chengang@gxmu.edu.cn

Yi-wu Dang
Department of Pathology, First Affiliated Hospital of Guangxi Medical University, 6 Shuangyong Road, Nanning, Guangxi 530021, People's Republic of China
Tel +0086-771-5356534
Fax +86 0771-5356534
Email dangyiwu@126.com

Introduction: MIR22HG has a reported involvement in the tumorigenesis of a variety of cancers, including hepatocellular carcinoma (HCC). However, the exact molecular mechanism of *MIR22HG* in HCC has not been clarified.

Methods: In the present study, we integrated data from in-house RT-qPCR, RNA-sequencing, microarray, and literature studies to conduct a comprehensive evaluation of the clinicopathological and prognostic significance of *MIR22HG* in an extremely large group of HCC samples. We also explored the potential mechanism of *MIR22HG* in HCC by analyzing the alteration profiles of *MIR22HG* in HCC to predict transcription factors (TFs) that may interact with *MIR22HG* and to annotate the biological functions of genes co-expressed with *MIR22HG*. *MIR22HG* expression was also compared in HCC nude mice xenografts before and after a treatment with nitidine chloride.

Results: We found that *MIR22HG* was downregulated in HCC and that this downregulation correlated with the malignant phenotype of HCC. Comprehensive analysis of the prognostic impact of *MIR22HG* in HCC revealed a beneficial effect of *MIR22HG* on the survival outcome of HCC patients. Seven cases of *MIR22HG* deep deletion occurred in 360 of the cancer genome atlas (TCGA) provisional HCC samples. A total of 22 *MIR22HG*-TF-mRNA triplets in HCC were predicted by the lncRNAmap. Co-expressed genes of *MIR22HG*, identified by weighted correlation network analysis (WGCNA), mainly participated in the pathways involving osteoclast differentiation, chemokine signaling pathways, and hematopoietic cell lineage. In vivo experiments demonstrated that nitidine chloride could stimulate *MIR22HG* expression in HCC xenografts.

Conclusion: In summary, *MIR22HG* may play a tumor-suppressive role in HCC by coordinating with predicted TFs and co-expressed genes, such as *NLRP3*, *CSF1R*, *SIGLEC10*, and *ZEB2*, or by being controlled by nitidine chloride.

Keywords: MIR22HG, hepatocellular carcinoma, RT-qPCR, transcription factor, co-expressed genes, nitidine chloride

Introduction

Liver cancer ranks sixth in cancer incidence worldwide and second in tumor-related mortality worldwide, with more than half of the new cases and deaths now being reported in China.[1] Hepatocellular carcinoma (HCC) is the predominant type of liver cancer and accounts for approximately 80% of liver cancer.[2] In the past decade, the incidence and mortality of HCC has shown an upward trend in both males and females.[3] Current treatment options for HCC patients include surgical resection, local ablation, and chemotherapy, and these have achieved certain

therapeutic effects. However, these treatment options also cause side effects, such as high recurrence rates after surgical resection and local ablation[4] and resistance to drugs, including sorafenib and regorafenib.[5–7] Therefore, identification of effective biomarkers and therapeutic strategies is imperative for improving the survival condition of HCC patients.

The rapid development of second-generation sequencing technology has raised awareness of epigenetic causes of human cancers. In particular, non-coding RNAs, such as long-chain non-coding RNAs (lncRNAs) have received wide attention. The lncRNAs are transcripts that are more than 200 nucleotides in length but cannot be translated into proteins.[8] These non-coding RNAs play important roles in diverse human cancers and affect tumor biology activities including ranging from cell proliferation and cell to apoptosis.[9–11] One lncRNA, *MIR22HG*, has a reported involvement in the tumorigenesis of a variety of cancers. For example, silencing of *MIR22HG* triggered apoptosis in lung cancer cells, while upregulation of *MIR22HG* inhibited the proliferation of endometrial cancer cells.[12,13] Studies have shown that overexpression of *MIR22HG* could significantly suppress the malignant progression of HCC, while indicating good survival outcome of HCC patients,[14–16] suggesting promising prospects for the application of *MIR22HG* in HCC treatment. Nevertheless, these studies had shortcomings, including the use of only limited numbers of HCC specimens for examining the expression level of *MIR22HG* in HCC and non-cancer tissues and the lack of sufficient diversity in the methods used to evaluate the expression of *MIR22HG* in HCC and non-cancer tissues. For these reasons, the exact molecular mechanism of *MIR22HG* in HCC has not yet been clarified.

In the present study, we performed a multidimensional assessment of the clinical significance of *MIR22HG* in an extremely large group of HCC samples by integrating data from in-house quantitative reverse transcription-polymerase chain reactions (qRT-PCR), RNA-sequencing, microarrays, and literature studies. Comprehensive indexes calculated from the present study, which included the standardized mean difference (SMD) and summarized receiver operating characteristic (SROC) curves, offered a relatively impartial evaluation of the differential expression of *MIR22HG* in HCC and non-cancer tissues. We also endeavored to uncover the molecular mechanism of *MIR22HG* in HCC by investigating the alterations in the profiles of *MIR22HG* in HCC, the transcription factors (TF) interacting with *MIR22HG*, the biological functions of the co-expressed genes of *MIR22HG*, and how nitidine chloride influences *MIR22HG* expression in HCC.

Materials And Methods

Clinico-Pathological Significance Of MIR22HG In HCC

In-House qRT-PCR

HCC and paired non-cancer tissues were collected from March 2018 to March 2019 from 101 HCC patients, aged between 35 and 68 years (12 male and 8 female), who were treated at the First Affiliated Hospital of Guangxi Medical University (Nanning, China). The samples were fixed in 10% buffered formalin for 16 h and then paraffin embedded. All enrolled patients signed informed consent forms, and the Ethics Committee of the First Affiliated Hospital of Guangxi Medical University approved the study.

Table 1 Information On The Primers For *MIR22HG* And *GAPDH*

	Sequence(5′->3′)	Template Strand	Length	Start	Stop	Tm	GC%	Self Complementarity	Self 3′ Complementarity
Forward primer for MIR22HG	CCAGTTGAAGAACTGTTGCCC	Plus	21	229	249	59.66	52.38	6.00	1.00
Reverse primer for MIR22HG Forward primer for GAPDH	CGTATCATCCACCCTGCTGT AGTGGCAAAGTGGAGATT	Minus	20	350	331	59.53	55	3.00	0.00
Reverse primer for GAPDH	GTGGAGTCATACTGGAACA								

Abbreviation: Tm, melting temperature.

The process of qRT-PCR has been described in detail in previous studies.[17–19] GAPDH served as the reference gene for *MIR22HG*. Information about the primers for *MIR22HG* and *GAPDH* is listed in Table 1.[18,19] MIR22HG expression was calculated by the formula:

$2-\Delta Cq = -(CqMIR22HG-CqGAPDH)$[20]

Evaluation Of The Clinicopathological Associations Of MIR22HG In HCC Using mRNA Data

In the present study, we obtained $\log_2(x+0.001)$-transformed level 3 transcripts per million reads (TPM) RNA-seq data from 374 HCC and 50 adjacent normal tissues, as well as the clinicopathological information, from The Cancer Genome Atlas (TCGA) data portal (https://portal.gdc.cancer.gov/) (IBM Corp., Armonk, NY, USA). An additional 175 normal liver tissues from Genotype-Tissue Expression (GTEx) (https://www.gtexportal.org/home/) were also included as the non-cancer control, giving mRNA-seq data from a total of 374 HCC and 225 non-cancer tissues.

Integrated SMD Of MIR22HG Expression In HCC And Non-Cancer Tissues

Microarrays published before July 18, 2019 and pertaining to expression data for *MIR22HG* in HCC and non-cancer tissues were searched in the GEO (https://www.ncbi.nlm.nih.gov/gds/) and ArrayExpress (https://www.ebi.ac.uk/arrayexpress/) databases using the search terms "(C17orf91 OR MIR22HG OR MIR22 host gene) AND (hepato OR liver OR hepatic OR HCC) AND (adenocarcinoma OR carcinoma OR cancer OR neoplasm OR tumor OR tumor OR neoplas OR malignan)". Studies were included if they offered sufficient *MIR22HG* expression data (more than five HCC or non-cancer cases) in human HCC and non-cancer samples for the calculation of a SMD. Basic information, as well as expression data and data used to plot SROC curves, were extracted from the included studies according to methods described previously.[21] Forest plots of SMDs with the 95% confidence interval (CI) were produced for in-house RT-qPCR

Table 2 Clinico-Pathological Value Of *MIR22HG* Expression In HCC From RT-qPCR Data

Clinico-Pathological Feature		N	MIR22HG Relevant Expression		
			M ± SD	t	P
Tissue	Cancer Non-cancer liver tissue	101 101	0.752 ± 0.838 4.058 ± 5.197	−6.313	<0.001
Gender	Male Female	80 21	0.707 ± 0.842 0.922 ± 0.823	−1.044	0.299
Age	≥50 <50	51 50	0.930 ± 1.023 0.570 ± 0.547	2.216	0.030
Metastasis	Yes No	52 49	0.480 ± 0.613 1.040 ± 0.949	3.540	<0.001
TNM	III-IV I-II	76 25	0.723 ± 0.843 0.839 ± 0.834	0.600	0.550
Embolus	Yes No	32 69	0.557 ± 0.512 0.842 ± 0.942	1.959	0.053
Nodes	Multiple Single	44 57	0.689 ± 0.850 0.800 ± 0.834	0.653	0.515
Vascular invasion	Yes No	38 63	0.512 ± 0.644 0.896 ± 0.911	2.479	0.015
Capsular	No Yes	52 49	0.720 ± 0.815 0.786 ± 0.870	0.394	0.695
Cirrhosis	Yes No	47 54	0.854 ± 0.922 0.662 ± 0.756	1.151	0.252

Notes: Unpaired and paired sample *t*-test was performed to evaluate the clinico-pathological parameters of HCC. P<0.05 was considered statistically significant.
Abbreviations: N, number; M, mean; SD, standard deviation.

data, mRNA-seq, and microarrays, as described previously.[21] A series of plots, including SROC, forest plots of sensitivity (SEN), specificity (SPE), positive likelihood ratio (PLR), negative likelihood ratio (NLR), and diagnostic odds ratio (DOR), were created using MetaDisc v.1.4.

Literature Study Selection For Comprehensive Analysis Of The Prognostic Value Of MIR22HG In HCC

In addition to the GEO and Arrayexpress databases, studies published as of July 18, 2019 were retrieved from literature databases, including PubMed, ScienceDirect, Ovid, Wiley Online Library, Web of Science, Springerlink, Embass, Chinese VIP, CNKI, Sinomed, and Wang Fang, to evaluate the prognostic significance of *MIR22HG* in HCC. The search terms for the literature searches were the same as those used for searching microarrays. Studies were included if they met the following requirements: (1) published in Chinese or English and (2) reporting sufficient data, including the hazard ratios (HRs) with 95% CIs for overall survival (OS) for HCC patients with different *MIR22HG* expression levels. Studies were excluded for the following reasons: (1) publication as letters, case reports, reviews, or conference reports and (2) incomplete prognostic data for *MIR22HG* in HCC. When duplicate study cohorts were encountered, only the most recent study was included. The first author, method for survival analysis, and HRs with 95% CIs were extracted from the qualified studies. HR values with 95% CIs for mRNA-seq, two microarrays

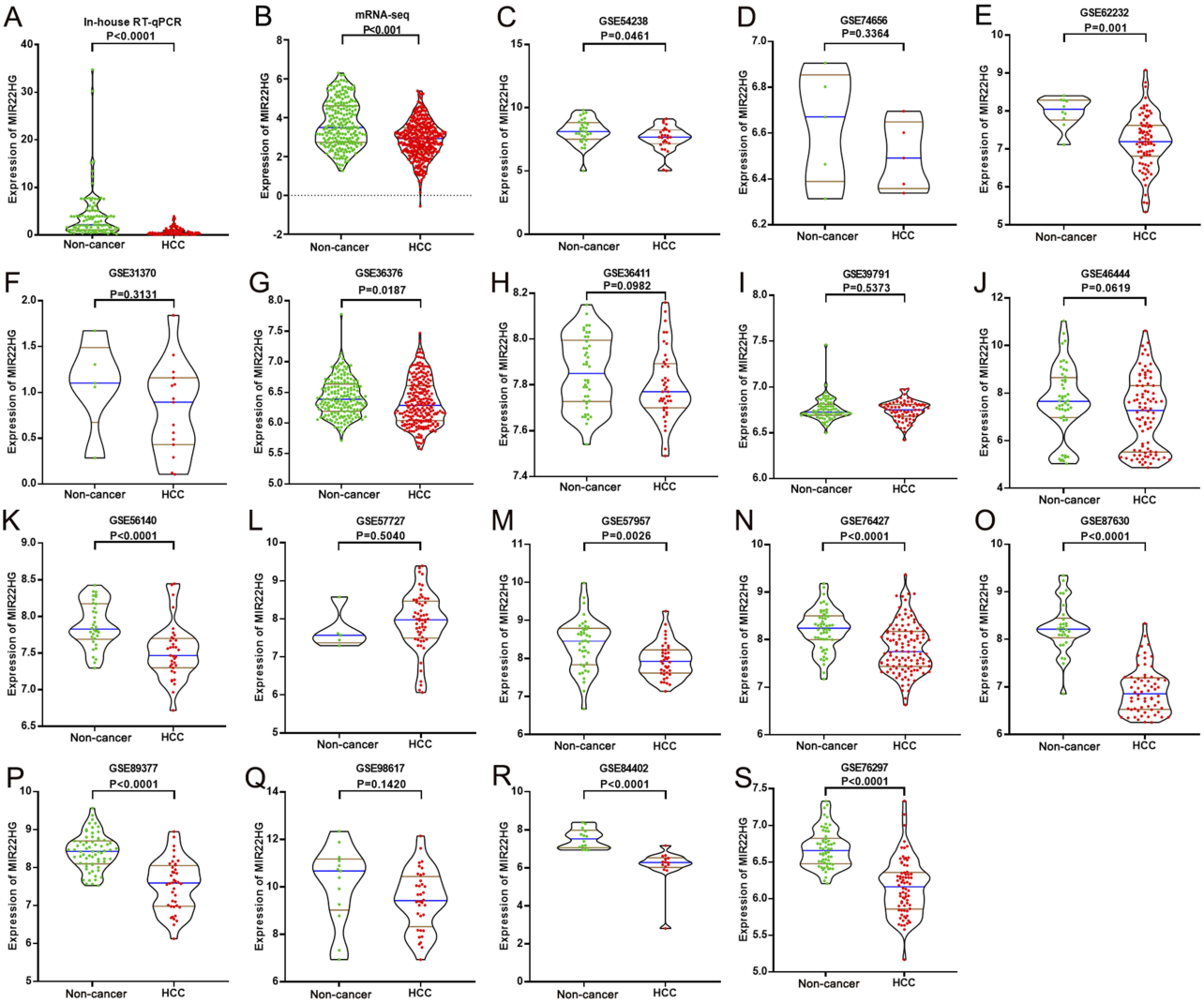

Figure 1 MIR22HG expression in in-house RT-qPCR, mRNA-seq, and 17 of the included microarrays Violin plots display the differential expression levels of *MIR22HG* in non-cancer samples and HCC samples for in-house RT-qPCR, mRNA-seq and 17 of the included microarrays (GSE54238, GSE74656, GSE62232, GSE31370, GSE36376, GSE36411, GSE39791, GSE46444, GSE56140, GSE57727, GSE57957, GSE76427, GSE87630, GSE89377, GSE98617, GSE84402, and GSE76297) **(A-S)**.

(GSE76427 and E-MTAB-36), and all the included literature studies were merged using the meta package of R software v.3.5.2.

Potential Molecular Mechanism Of MIR22HG In HCC

Gene Alteration Of MIR22HG In HCC Tissue From cBioPortal

The cBioPortal database (http://www.cbioportal.org) was mined for mutation profiles of *MIR22HG* in HCC.[22] The alteration status of *MIR22HG* in 440 TCGA provisional HCC samples was queried from the OncoPrint module of cBioPortal.

Predicting MIR22HG–TF-mRNA Triplets In HCC

The interaction between TFs and lncRNAs contributed partly to the driving mechanism of HCC; therefore, we hypothesized that TFs might be involved in *MIR22HG*-related tumorigenesis of HCC. TFs that potentially could bind to *MIR22HG* were predicted through

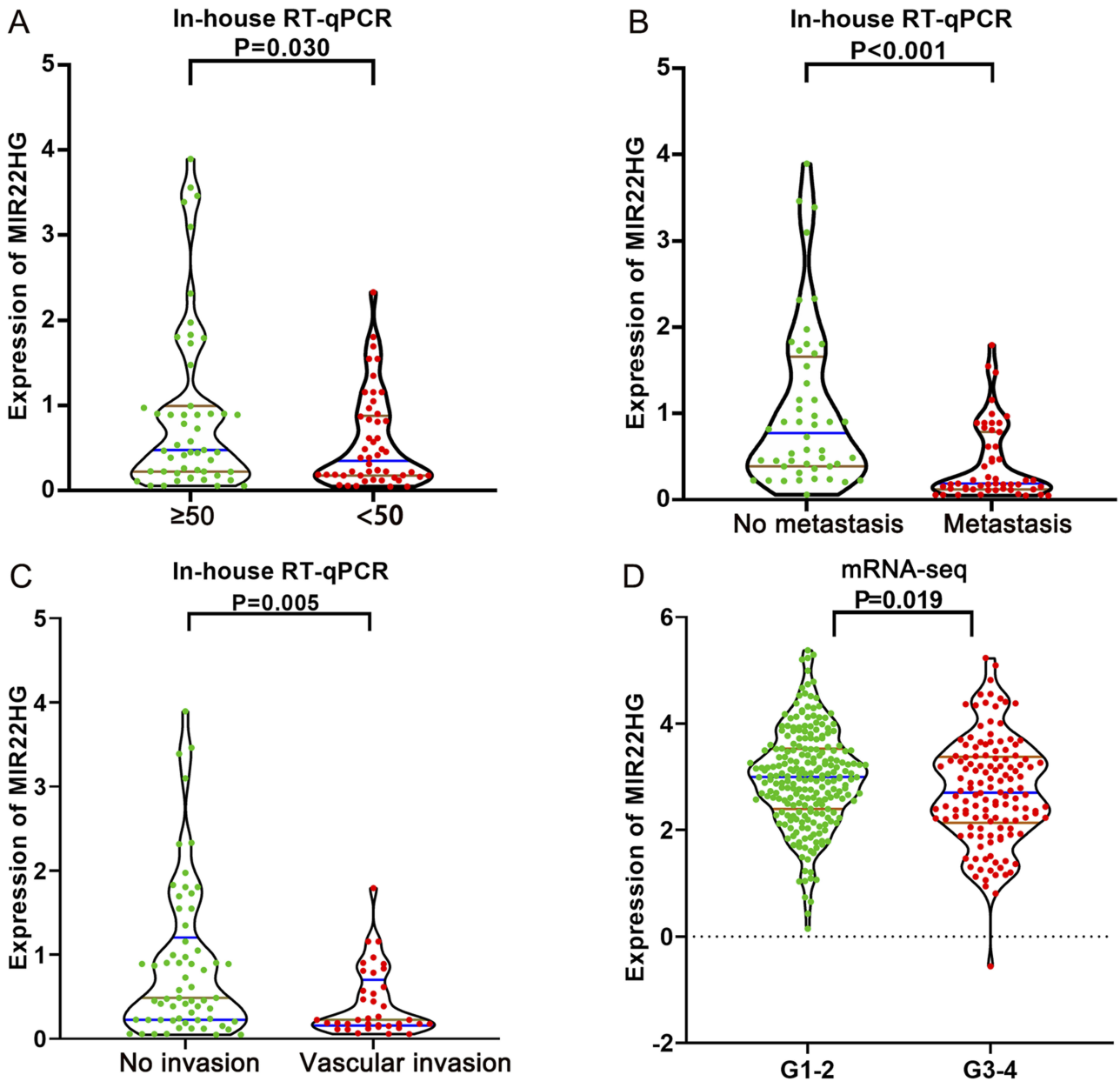

Figure 2 Distribution of *MIR22HG* in different groups of clinical features (**A**) MIR22HG expression in groups of different ages from in-house RT-qPCR; (**B**) Metastasis status from in-house RT-qPCR; (**C**) Vascular invasion status from in-house RT-qPCR; (**D**) Clinical grades from mRNA-seq data.

lncRNAMap. Correlation between the log2 (x+0.001) transformed transcripts per million (TPM) expression of *MIR22HG* and the predicted TFs in TCGA-HCC cohorts was assessed by Pearson correlation analysis in Graphpad Prism v.8.0.

Co-Expression Analysis Of MIR22HG

We first calculated the differentially expressed genes (DEGs) based on the count data of 374 HCC and 50 adjacent normal samples from TCGA, which was performed using the limma voom package of R software v.3.5.2.[23] Genes with a log2 fold change value >1 or <1 and an adjusted P value <0.01 were defined as DEGs. We integrated the log2 (x+0.001) TPM expression value of DEGs and *MIR22HG* in 374 TCGA-HCC samples into an input matrix for subsequent co-expression analysis. Weighted correlation network analysis (WGCNA) was carried out utilizing the WGCNA package in R software v.3.5.2 for identification of genes that were co-expressed with *MIR22HG*. A co-expression network of *MIR22HG* and co-expressed genes was constructed in Cytoskape v.3.7 according to the calculated weight value of more than 0.05. We then analyzed the biological functions, pathways, and disease enrichment of the co-expressed genes using the ClusterProfiler package in R software v.3.5.2. Terms with P value < 0.05 were considered statistically significant.

The Impact Of Nitidine Chloride On Expression Of MIR22HG In HCC

Our team is researching the anti-cancer effect and mechanism of traditional Chinese medicines. Specifically, considerable research data have been accumulated for nitidine chloride, and we have found an inhibitory effect of nitidine chloride on the growth of liver cancer cells.[24,25] Taking into account the clinico-pathological action of *MIR22HG* in HCC, we hypothesized that it might be affected by traditional Chinese medicines such as nitidine chloride. Therefore, we performed in vivo experiments on nude mice to investigate the influence of nitidine chloride on

Table 3 Clinico-Pathological Value Of *MIR22HG* Expression In HCC From mRNA-Seq Data

Clinico-Pathological Feature		**N**	**MIR22HG Relevant Expression**		
			M ± SD	**t**	**P**
Tissue	Cancer	374	2.879 ± 0.948	−8.63	<0.001
	Normal	225	3.678 ± 1.179		
Gender	MALE	250	2.860 ± 0.954	−0.872	0.384
	FEMALE	121	2.951 ± 0.927		
Age	>60	193	2.957 ± 0.904	1.514	0.131
	≤60	177	2.808 ± 0.981		
Stage	III-IV	90	2.733 ± 1.035	1.486	0.138
	I-II	257	2.904 ± 0.905		
M stage	M1	4	2.009 ± 0.619	1.648	0.101
	M0	266	2.814 ± 0.973		
N stage	N1	4	3.330 ± 1.497	−1.071	0.285
	N0	252	2.808 ± 0.960		
T stage	T3-4	93	2.746 ± 0.993	1.647	0.100
	T0-2	275	2.932 ± 0.926		
Grade	G3-4	134	2.734 ± 0.991	2.365	0.019
	G1-2	232	2.976 ± 0.912		

Notes: Unpaired sample *t* test was performed to evaluate the clinico-pathological parameters of HCC. P<0.05 was considered statistically significant.
Abbreviations: N, number; M, mean; SD, standard deviation.

Table 4 Basic Information For All Included Microarrays

Number	Study	Cancer N	Cancer M	Cancer SD	Non-Cancer N	Non-Cancer M	Non-Cancer SD	Sample Type	Platform	Experiment
1	GSE54238	26	7.585	1.004	30	8.134	1.003	Tissue	GPL16955	Non-coding RNA profiling by array
2	GSE74656	5	6.501	0.150	5	6.632	0.243	Tissue	GPL16043	Expression profiling by array
3	GSE31370	15	0.816	0.497	5	1.084	0.509	Tissue	GPL10558	Expression profiling by array
4	GSE36376	240	6.339	0.374	193	6.417	0.302	tissue	GPL10558	Expression profiling by array
5	GSE36411	42	7.799	0.152	42	7.855	0.155	Tissue	GPL10558	Expression profiling by array
6	GSE39791	72	6.744	0.108	72	6.756	0.126	Tissue	GPL10558	Expression profiling by array
7	GSE46444	88	7.149	1.515	48	7.660	1.511	Tissue	GPL13369	Expression profiling by array
8	GSE56140	35	7.525	0.383	34	7.885	0.307	Tissue	GPL18461	Expression profiling by array
9	GSE57727	57	7.932	0.754	5	7.700	0.505	Tissue	GPL14951	Expression profiling by array
10	GSE57957	39	7.955	0.464	39	8.346	0.681	Tissue	GPL10558	Expression profiling by array
11	GSE76427	115	7.823	0.518	52	8.210	0.437	Tissue	GPL10558	Expression profiling by array
12	GSE87630	64	6.918	0.482	30	8.248	0.527	Tissue	GPL6947	Expression profiling by array
13	GSE89377	40	7.536	0.670	67	8.419	0.463	Tissue	GPL6947	Expression profiling by array
14	GSE98617	36	9.458	1.252	13	10.116	1.635	Tissue	GPL14951	Expression profiling by array
15	GSE84402	14	6.089	1.001	14	7.539	0.516	Tissue	GPL570	Expression profiling by array
16	GSE76297	74	6.160	0.385	58	6.683	0.259	Tissue	GPL17586	Expression profiling by array
17	GSE62232	81	7.203	0.712	10	7.983	0.389	Tissue	GPL570	Expression profiling by array
18	GSE60502	18	8.923	0.691	18	9.971	0.607	Tissue	GPL96	Expression profiling by array
19	GSE46408	6	9.069	0.362	6	9.788	0.378	Tissue	GPL4133	Expression profiling by array
20	GSE45436	93	6.115	0.929	41	7.236	0.693	Tissue	GPL570	Expression profiling by array
21	GSE45267	46	5.975	0.725	41	7.111	0.712	Tissue	GPL570	Expression profiling by array
22	GSE25097	268	1.179	0.863	289	2.450	1.169	Tissue	GPL10687	Expression profiling by array
23	GSE14520-GPL571	22	6.123	0.636	21	7.481	0.479	Tissue	GPL571	Expression profiling by array
24	GSE25599	13	13.248	8.848	13	14.086	2.516	Tissue	GPL9052	Expression profiling by high throughput sequencing
25	GSE77314	50	10.268	7.812	50	25.975	11.265	Tissue	GPL9052	Expression profiling by high throughput sequencing
26	GSE124535	35	7.920	4.562	35	8.205	3.125	Tissue	GPL20795	Expression profiling by high throughput sequencing
27	GSE94660	21	1.873	0.717	21	2.394	0.544	Tissue	GPL16791	Expression profiling by high throughput sequencing
28	GSE56545	30	8.114	1.100	29	9.878	0.860	Tissue	GPL15433	Expression profiling by high throughput sequencing

(*Continued*)

Table 4 (Continued).

Number	Study	Cancer N	Cancer M	Cancer SD	Non-Cancer N	Non-Cancer M	Non-Cancer SD	Sample Type	Platform	Experiment
29	GSE87592	27	20.027	18.222	26	19.245	10.371	Tissue	GPL11154	Expression profiling by high throughput sequencing
30	GSE65485	50	5.280	3.005	5	8.898	2.688	Tissue	GPL11154	Expression profiling by high throughput sequencing
31	GSE69164	11	6.476	1.964	11	11.552	6.135	Tissue	GPL11154	Expression profiling by high throughput sequencing
32	GSE63863	12	6.117	2.247	12	11.377	5.880	Tissue	GPL11154	Expression profiling by high throughput sequencing
33	GSE82177	8	7.502	2.452	19	9.104	5.002	Tissue	GPL11154	Expression profiling by high throughput sequencing
34	GSE14520-GPL3921	225	6.389	0.768	220	7.540	0.507	Tissue	GPL3921	Expression profiling by array
35	E-MTAB-1503	7	7.038	0.617	10	7.923	0.876	Cells	HG-U133_Plus_2	Transcription profiling by array
36	E-TABM-36	57	6.056	0.584	5	6.755	0.218	Tissue	HG-U133A	Transcription profiling by array
37	E-MTAB-950	119	7.460	0.834	157	8.034	0.889	Tissue	HG-U133_Plus_2	Transcription profiling by array

Abbreviations: N, number; M, mean; SD, standard deviation.

MIR22HG expression in HCC. Male and female nude mice, purchased from Shanghai SLAC Laboratory Animal Co., Ltd. (Shanghai, China), were handled according to the Guide for the Care and Use of Laboratory Animals (the Shanghai SLAC Laboratory Animal of China, 2015). Each mouse was inoculated with SMMC7721 cells (1×10^7 cells/mL, 0.2mL in total) by subcutaneous injection into the right armpit. When the injected cells had produced a tumor of approximately 70 mm^3 in size, all mice were randomly assigned to either the negative control group for intraperitoneal injection with saline or the treatment group for injection with 7 mg/kg nitidine chloride. After 15 days, the mice were anesthetized, and the tumor tissues were excised and stored at −80°C.

Total RNA was extracted with TRIzol Regent (Invitrogen, USA). RNA purity was determined using the NanoPhotometer® spectrophotometer (IMPLEN, CA, USA). RNA integrity was checked using the RNA Nano 6000 Assay Kit of the Agilent Bioanalyzer 2100 system (Agilent Technologies, CA, USA).

The mRNA sequencing libraries were established using the rRNA-depleted RNA and the NEB Next® Ultra™ Directional RNA Library Prep Kit for Illumina® (NEB, USA), following the manufacturer's recommendations. The library quality was checked using the Agilent Bioanalyzer 2100 system. After removing reads with adaptors, >5% unknown nucleotides, and low-quality bases, the qualified reads were mapped against human genome references (GRCh37/hg19). Differentially expressed lncRNAs were identified based on the count data of lncRNAs using DESeq2 package in R software v.3.3.2 ($|\log2FC|>1$, $P<0.01$).

Statistical Analysis

SPSS 22.0 was used for the statistical analyses of mRNA-seq and RT-qPCR data. The expression data for *MIR22HG* are presented as M ± SD. The expression levels of *MIR22HG* in HCC and non-cancer tissues determined by RT-qPCR were evaluated by paired sample *t*-tests and *MIR22HG* expression levels in HCC and non-cancer tissues from mRNA-seq were evaluated by independent samples *t*-tests. The significance of differential *MIR22HG* expression between two groups with different clinicopathological parameters was examined by independent samples *t*-tests. ROC curves were plotted to assess the discriminatory value of *MIR22HG* for HCC. AUC values of 0.5–0.7, 0.7–0.9, and 0.9–1.0 indicated a poor, moderate, and high discriminatory capacity, respectively. The prognostic significance of *MIR22HG* for HCC was examined by dividing all patient samples from mRNA-seq or microarrays (GSE76427 and E-MTAB-36) into two groups according to the median expression level of *MIR22HG*. Kaplan–Meier survival curves were drawn to compare the survival condition of patients with high or low *MIR22HG* expression. A P-value of less than 0.05 was considered statistically significant.

Table 5 Data Used To Plot The sROC Curves From All Included Microarrays

Accession Number	TP	FP	FN	TN
GSE54238	26	29	0	1
GSE74656	5	4	0	1
GSE31370	1	0	14	5
GSE36376	34	19	206	174
GSE36411	2	1	40	41
GSE39791	45	36	27	36
GSE46444	82	44	6	4
GSE56140	2	0	33	34
GSE57727	41	1	16	4
GSE57957	39	38	0	1
GSE76427	1	0	114	52
GSE87630	64	30	0	0
GSE89377	40	67	0	0
GSE98617	35	11	1	2
GSE84402	14	14	0	0
GSE76297	1	0	73	58
GSE62232	3	0	78	10
GSE60502	18	18	0	0
GSE46408	6	6	0	0
GSE45436	93	41	0	0
GSE45267	46	41	0	0
GSE25097	268	289	0	0
GSE14520-GPL571	22	21	0	0
GSE25599	13	13	0	0
GSE77314	50	50	0	0
GSE124535	13	8	22	27
GSE94660	21	21	0	0
GSE56545	30	29	0	0
GSE87592	24	20	3	6
GSE65485	1	0	49	5
GSE69164	11	11	0	0
GSE63863	12	12	0	0
GSE82177	5	10	3	9
GSE14520_GPL3921	225	220	0	0
E-MTAB-1503	5	0	5	7
E-TABM-36	24	5	33	0
E-MTAB-950	119	157	0	0

Abbreviations: TP, true positivity; FP, false positivity; FN, false negativity; TN, true negativity.

Results

Clinico-Pathological Significance Of MIR22HG In HCC

Differential Expression Of MIR22HG In HCC And Non-Cancer Tissues

Statistical analysis of RT-qPCR data for 101 HCC and paired non-cancer tissues demonstrated a significant downregulation of *MIR22HG* in HCC tissues compared with non-cancer tissues (P<0.001) (Table 2, Figure 1). The expression of *MIR22HG* was also inversely correlated with metastasis and vascular invasion (P<0.001 and P = 0.015) (Table 2, Figure 2). MRNA-seq data for 374 HCC and 225 non-cancer samples also revealed the significant downregulation of *MIR22HG* in HCC (P<0.001) (Table 3) (Figure 1). A difference was also detected in the *MIR22HG* expression in groups of TCGA-HCC patients with various grades. Patients with advanced grade HCC (III–IV) had significantly lower expression of *MIR22HG* when compared with patients with early grade HCC (I–II) (Table 3, Figure 2).

The GEO and Arrayexpress searches retrieved a total of 34 GEO microarrays and three Arrayexpress

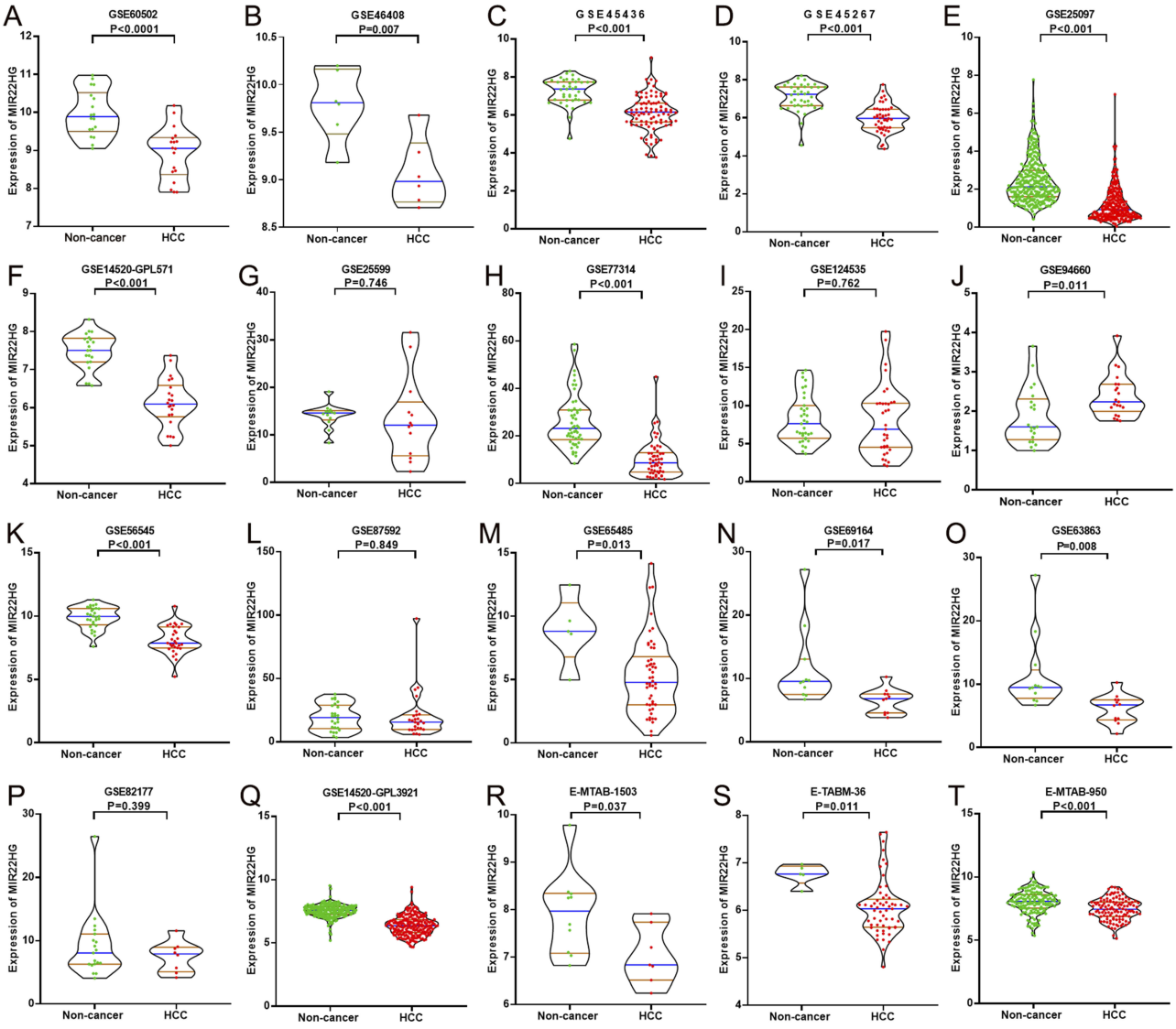

Figure 3 MIR22HG expression in 20 of the included microarrays Violin plots display the differential expression levels of *MIR22HG* in non-cancer samples and HCC samples for 20 of the included microarrays (GSE60502, GSE46408, GSE45436, GSE45267, GSE25097, GSE14520-GPL571, GSE25599, GSE77314, GSE124535, GSE94660, GSE56545, GSE87592, GSE65485, GSE69164, GSE63863, GSE82177, GSE14520_GPL3921, E-MTAB-1503, E-TABM-36, and E-MTAB-950) (**A-T**).

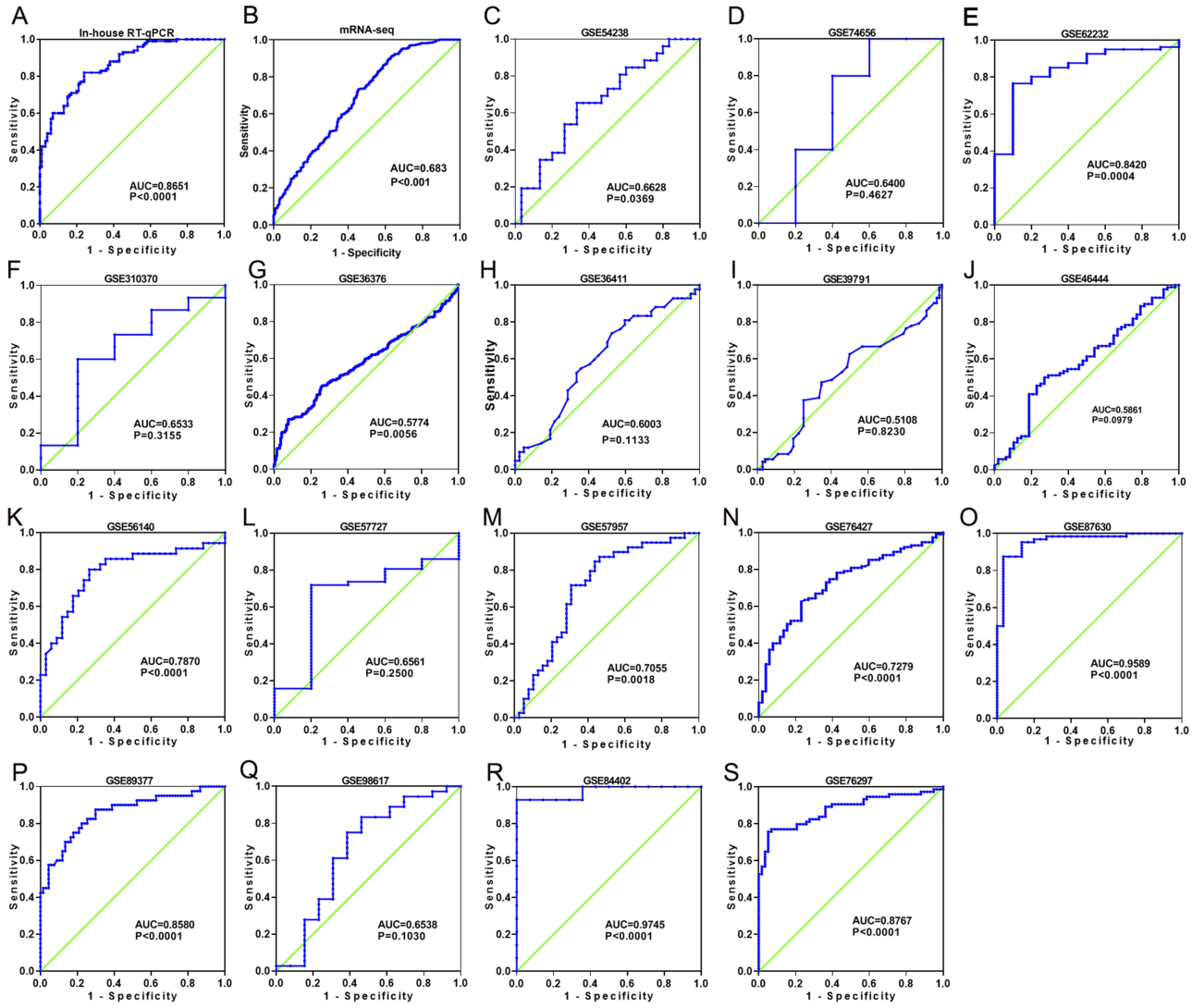

Figure 4 Discriminatory ability of *MIR22HG* in hepatocellular carcinoma (HCC) for in-house RT-qPCR, mRNA-seq, and part of the included microarrays A panel of ROC curves shows the discriminatory capacity of *MIR22HG* for HCC in in-house RT-qPCR, mRNA-seq, and part of the included microarrays (**A-S**).

microarrays with sufficient expression data for *MIR22HG* in more than five HCC and non-cancer samples; these were considered eligible for the integrated calculation of SMD. The basic information and extracted data for all the included microarrays is summarized in Tables 4 and 5. *MIR22HG* showed a clearly downregulated expression in most of the microarrays (P<0.05) (Figures 1 and 3). A panel of ROC curves for the in-house RT-qPCR, mRNA-seq, and all included microarrays suggested a good ability of *MIR22HG* to distinguish HCC from non-cancer tissues (Figures 4 and 5). The integrated SMD for the in-house RT-qPCR, mRNA-seq, and all included microarrays, which together covered an extremely large sample of 2636 HCC and 2072 non-cancer samples, corroborated the downregulated expression of *MIR22HG* in HCC (SMD = −0.97, 95% CI = −1.17- −0.77, I^2 = 88%, P<0.01) (Figure 6). Subgroup analysis revealed that experiment type might be a potential source of heterogeneity because the microarrays in the subgroup of transcription profiling by array showed no heterogeneity (I^2 = 0%, P = 0.42) (Figure 6B). The sROC curves and forest plots of SEN, SPE, PLR, NLR, and DOR for in-house RT-qPCR, mRNA-seq and all included microarrays confirmed the moderate capability of *MIR22HG* to differentiate HCC from non-cancer tissues (Figure 7).

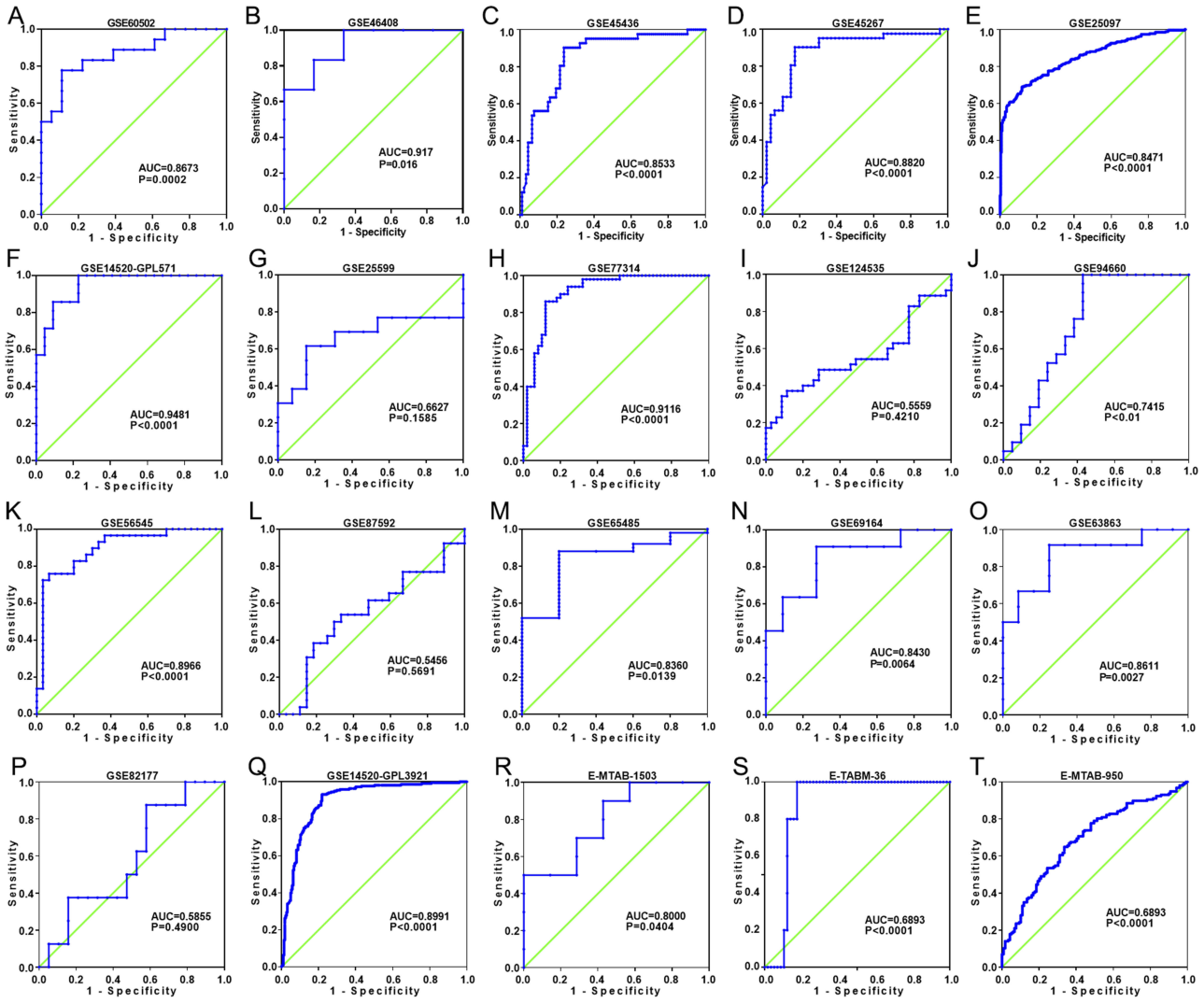

Figure 5 Discriminatory ability of *MIR22HG* in hepatocellular carcinoma (HCC) for the other part of the included microarrays A panel of ROC curves shows the discriminatory capacity of *MIR22HG* for HCC in the other part of the included microarrays (**A-T**).

The Prognostic Impact Of MIR22HG On HCC

Kaplan-Meier survival curves were plotted for mRNA-seq data and two microarray studies (GSE76427 and E-MTAB-36) containing overall survival data for *MIR22HG* in HCC (Figure 8). Three literature studies that provided overall survival data of *MIR22HG* were enrolled for comprehensive analysis of the prognostic significance of *MIR22HG* for HCC.[15,16,26] Survival data extracted from the three included literature studies are listed in Table 6. Pooled HRs incorporating overall survival data from mRNA-seq, two microarrays, and three literature studies implicated *MIR22HG* as a protective prognostic factor for HCC (HR = 0.75, 95% CI = 0.64–0.89, I^2 = 64%, P<0.01) (Figure 9A). Subgroup analysis and sensitivity analysis reported an unspecified cause of heterogeneity (Figure 9B and C). No significant publication bias was detected in the symmetrical funnel plot (P = 0.517) (Figure 9D).

Potential Molecular Mechanism Of MIR22HG In HCC

Gene Alteration Of MIR22HG In HCC Tissue From cBioPortal

Alteration profiles in cBioPortal indicated the occurrence of 18 cases of gene alteration, including two cases of amplification, seven cases of deep deletion, and nine cases of high mRNA, in TCGA provisional HCC samples, accounting for 5% of all the profiled cases (Figure 11A).

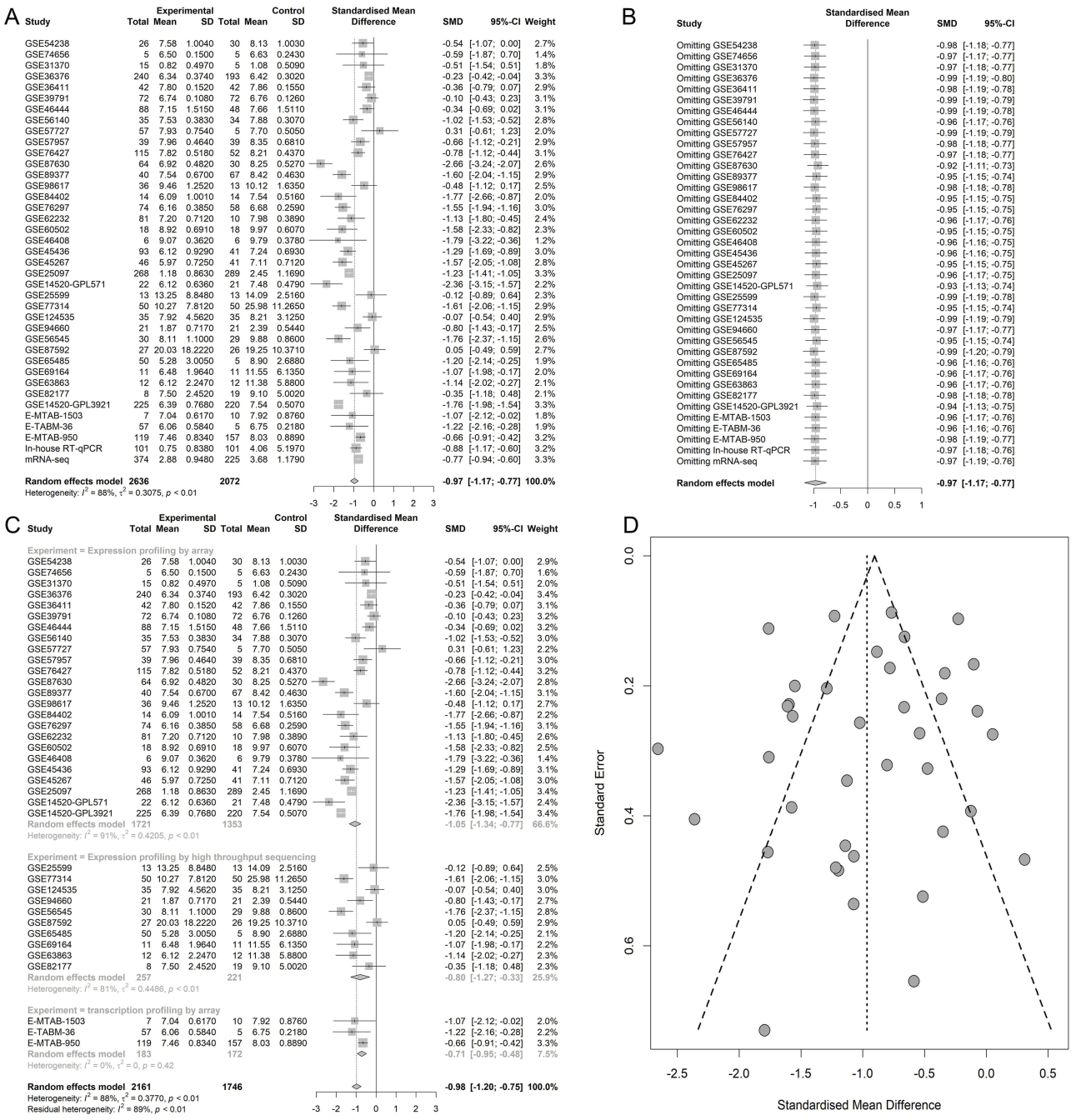

Figure 6 The integrated standardized mean difference (SMD) of *MIR22HG* expression in hepatocellular carcinoma (HCC) (**A**) Forest plot. (**B**) Sensitivity analysis. (**C**) Forest plot for the subgroup analysis. (**D**) Funnel plot.

Predicting MIR22HG-Transcription Factor (TF)-mRNA Triplets In HCC

A total of 22 *MIR22HG*-TF-mRNA triplets were predicted by lncRNAmap (Table 7). Of the 22 TFs with potential relationships with *MIR22HG*, we found significant reverse correlation between *MIR22HG* and HNF4A expression (r = −0.097, P = 0.045) (Figure 11B).

Co-Expression Analysis Of MIR22HG

In total, 5942 DEGs were identified by limma voom analysis in TCGA-LIHC cohorts. The WGCNA for the expression matrix of these DEGs and *MIR22HG* showed co-expression of 59 genes with *MIR22HG* (weight value >0.05) (Figure 12). Gene ontology (GO) and Kyoto Encyclopedia of Genes and Genomes (KEGG) analysis

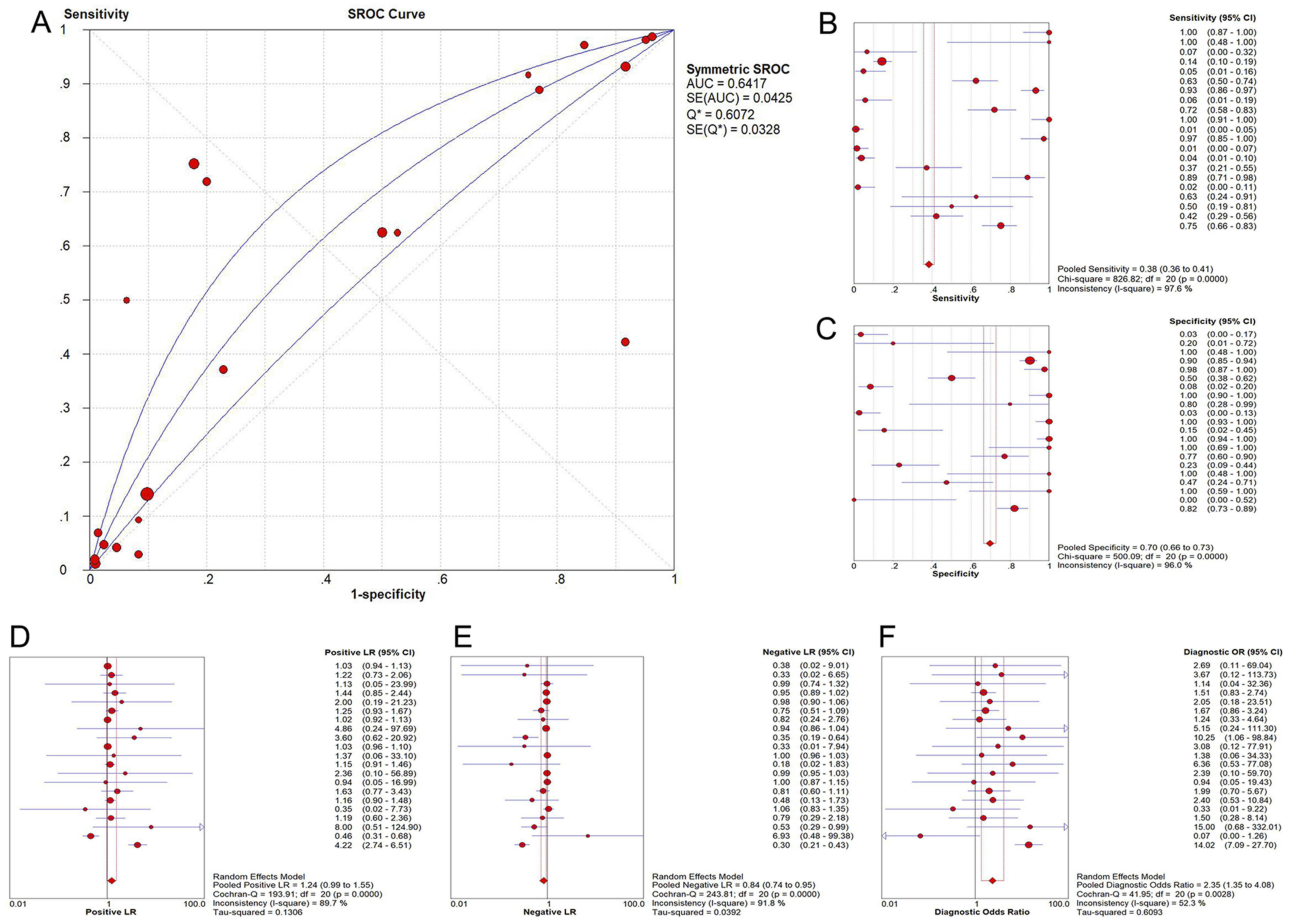

Figure 7 Summarized receiver operating characteristic (SROC) curves for in-house RT-qPCR, mRNA-seq, and all included microarrays (**A**) SROC curves; (**B**) Forest plot of sensitivity; (**C**) Forest plot of specificity; (**D**) Forest plot of positive likelihood ratio; (**E**) Forest plot of negative likelihood ratio; (**F**) Forest plot of diagnostic odds ratio.

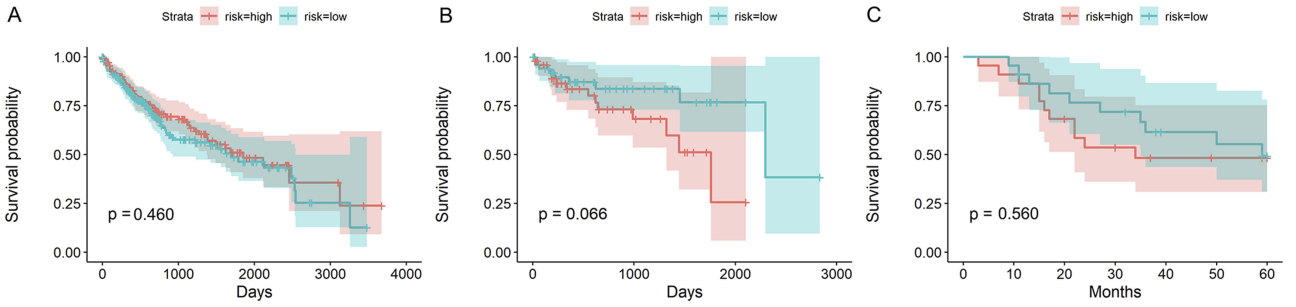

Figure 8 Kaplan-Meier survival curves of *MIR22HG* for mRNA-seq and two microarray studies (**A**) Survival condition for patients from mRNA-seq group; (**B**) Survival condition for patients from GSE76427; (**C**) Survival condition for patients from E-MTAB-36.

for co-expressed genes of *MIR22HG* disclosed their main enrichment in molecular functions that included protein tyrosine kinase activity, non-membrane spanning protein tyrosine kinase activity, and phosphotyrosine residue binding, as well as clustering in pathways that included osteoclast differentiation, chemokine signaling pathways, and hematopoietic cell lineage (P<0.05) (Figures 13A-C and 14). The co-expressed genes were associated with several diseases, including human immunodeficiency virus infectious disease, gout, and primary immunodeficiency disease (P<0.05) (Figure 13D).

Table 6 Summary Of Survival Data For The Comprehensive Prognostic Value Of *MIR22HG* In Hepatocellular Carcinoma (HCC)

Study	Year	HR	LCI	UCI	Method
Dong et al.	2017	0.952380952	0.528541226	0.931966449	Multivariate Cox regression analysis
Dong et al.	2018	0.510986203	0.381533766	0.692520776	Univariate Cox regression analysis
Zhang et al.	2018	0.496	0.27	0.912	Multivariate Cox regression analysis
Zhang et al.	2018	0.409	0.227	0.735	Univariate Cox regression analysis
Wu et al.	2018	0.79	0.68	0.92	Multivariate Cox regression analysis
Wu et al.	2018	0.8	0.68	0.94	Univariate Cox regression analysis
MRNA-seq	2017	0.889563224	0.735481157	1.075925226	Univariate Cox regression analysis
GSE76427	2018	1.63637116	0.767858135	3.487246475	Univariate Cox regression analysis
E-TABM-36	2014	0.765710262	0.373627176	1.569244002	Univariate Cox regression analysis

Abbreviations: HR, hazard ratio; LCI, lower confidence interval; UCI, upper confidence interval.

Differentially Expressed lncRNAs In Nitidine Chloride Treated HCC Xenografts

After the quality control of principal component analysis, two NC-treated and three control HCC xenograft tumor tissues were collected for detection of differentially expressed lncRNAs. The tumor volumes in the NC-treated group were significantly reduced compared with those of control group (p-value < 0.05).[27] Heatmaps for differentially expressed lncRNAs before and after the nitidine chloride treatment in HCC xenografts showed a significant upregulation of 23 lncRNAs and downregulation of 12 lncRNAs. In particular, *MIR22HG* was significantly upregulated in nitidine chloride-treated HCC xenograft tissues (log2FC = 1.373, P<0.001) (Figure 10).

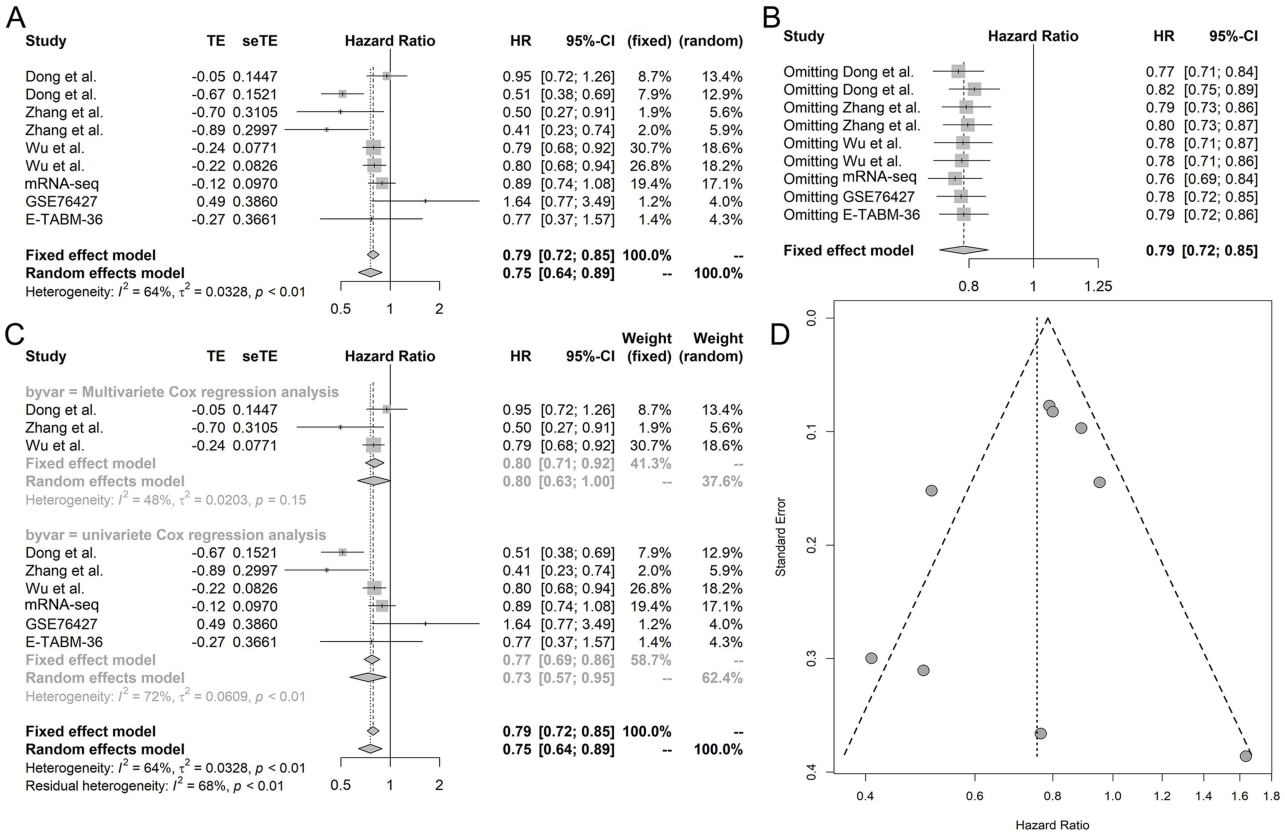

Figure 9 Comprehensive analysis of the prognostic value of *MIR22HG* in hepatocellular carcinoma (HCC) (**A**) Forest plot; (**B**) Sensitivity analysis; (**C**) Subgroup analysis based on methods; (**D**) Funnel plot.

Table 7 Predicted *MIR22HG*-TF-mRNA Triplets In Hepatocellular Carcinoma (HCC) From LncMAP

LncRNA ID	TF ID	TF Symbol	Gene ID	Gene Symbol	Correlation Coefficient In lncRNA Low Expression Group	Correlation Coefficient In lncRNA High Expression Group	Score	P value	FDR
ENSG00000186594	ENSG00000005339	CREBBP	ENSG00000052795	FNIP2	0.76	0.262	0.999	0	0
ENSG00000186594	ENSG00000028277	POU2F2	ENSG00000096968	JAK2	0.148	0.684	0.999	0	0
ENSG00000186594	ENSG00000036549	ZZZ3	ENSG00000108298	RPL19	−0.582	−0.0703	0.995	0	0
ENSG00000186594	ENSG00000077463	SIRT6	ENSG00000169756	LIMS1	−0.674	−0.198	0.996	0	0
ENSG00000186594	ENSG00000100393	EP300	ENSG00000052795	FNIP2	0.818	0.33	1	0	0
ENSG00000186594	ENSG00000101076	HNF4A	ENSG00000048740	CELF2	0.101	−0.597	1	0	0
ENSG00000186594	ENSG00000109320	NFKB1	ENSG00000005100	DHX33	0.699	0.223	0.997	0	0
ENSG00000186594	ENSG00000113580	NR3C1	ENSG00000197958	RPL12	−0.721	−0.185	0.999	0	0
ENSG00000186594	ENSG00000120837	NFYB	ENSG00000160957	RECQL4	−0.603	−0.081	0.996	0	0
ENSG00000186594	ENSG00000130522	JUND	ENSG00000118816	CCNI	−0.605	−0.0406	0.998	0	0
ENSG00000186594	ENSG00000137265	IRF4	ENSG00000118308	LRMP	0.225	0.693	0.997	0	0
ENSG00000186594	ENSG00000140262	TCF12	ENSG00000005100	DHX33	0.896	0.394	1	0	0
ENSG00000186594	ENSG00000147133	TAF1	ENSG00000065559	MAP2K4	0.551	0.0903	0.987	0	0
ENSG00000186594	ENSG00000154727	GABPA	ENSG00000111252	SH2B3	0.572	0.097	0.991	0	0
ENSG00000186594	ENSG00000156127	BATF	ENSG00000000938	FGR	0.105	0.667	0.999	0	0
ENSG00000186594	ENSG00000158773	USF1	ENSG00000170340	B3GNT2	−0.571	−0.0948	0.991	0	0
ENSG00000186594	ENSG00000169016	E2F6	ENSG00000079462	PAFAH1B3	0.277	0.814	1	0	0
ENSG00000186594	ENSG00000169083	AR	ENSG00000106560	GIMAP2	0.585	0.114	0.991	0	0
ENSG00000186594	ENSG00000169375	SIN3A	ENSG00000052795	FNIP2	0.605	0.0142	0.999	0	0
ENSG00000186594	ENSG00000170345	FOS	ENSG00000020633	RUNX3	0.0653	0.597	0.997	0	0
ENSG00000186594	ENSG00000184634	MED12	ENSG00000077348	EXOSC5	−0.538	−0.00149	0.995	0	0
ENSG00000186594	ENSG00000185591	SP1	ENSG00000005100	DHX33	0.748	0.12	1	0	0

Abbreviations: TF, transcription factor; FDR, false discovery rate.

Discussion

The novelties of this article are reflected in the following aspects. We integrated data from in-house RT-qPCR, RNA-sequencing, microarray, and literature studies to provide a comprehensive evaluation of the clinicopathological and prognostic significance of *MIR22HG* in an extremely large group of HCC samples. We explored the potential mechanism of *MIR22HG* in HCC by analyzing the alteration profiles of *MIR22HG* in HCC, by predicting TFs interacting with *MIR22HG*, and by annotating the biological functions of genes co-expressed with *MIR22HG*. We also compared the expression of *MIR22HG* in HCC nude mice xenografts before and after a treatment with nitidine chloride.

When our study is compared with several previous studies that explored the role of *MIR22HG* in HCC using a single method, one of the highlights of our study is that we conducted a comprehensive appraisal of the clinical significance of *MIR22HG* in HCC using an extremely large number of samples (2636 HCC and 2072 non-cancer tissues) collected from in-house RT-qPCR, RNA-seq, microarrays, and literature studies. The huge size of our sample group strengthened the reliability of our results. We confirmed downregulation of *MIR22HG* in HCC, the correlation between *MIR22HG* expression and the malignant phenotype of HCC, and the beneficial prognostic influence of *MIR22HG* on HCC, in agreement with the reports by prior research groups.[14–16] These results implied that downregulation of *MIR22HG* results in a loss of its protective effect in HCC and subsequent malignant progression of the tumor, which is no longer restrained by *MIR22HG*. Consequently, HCC patients with low *MIR22HG* expression are predicted to show worse survival.

The finding that *MIR22HG* is downregulated in HCC then raises the question of the nature of the mechanism directing the *MIR22HG* effects on HCC. Previous studies revealed that *MIR22HG* could regulate

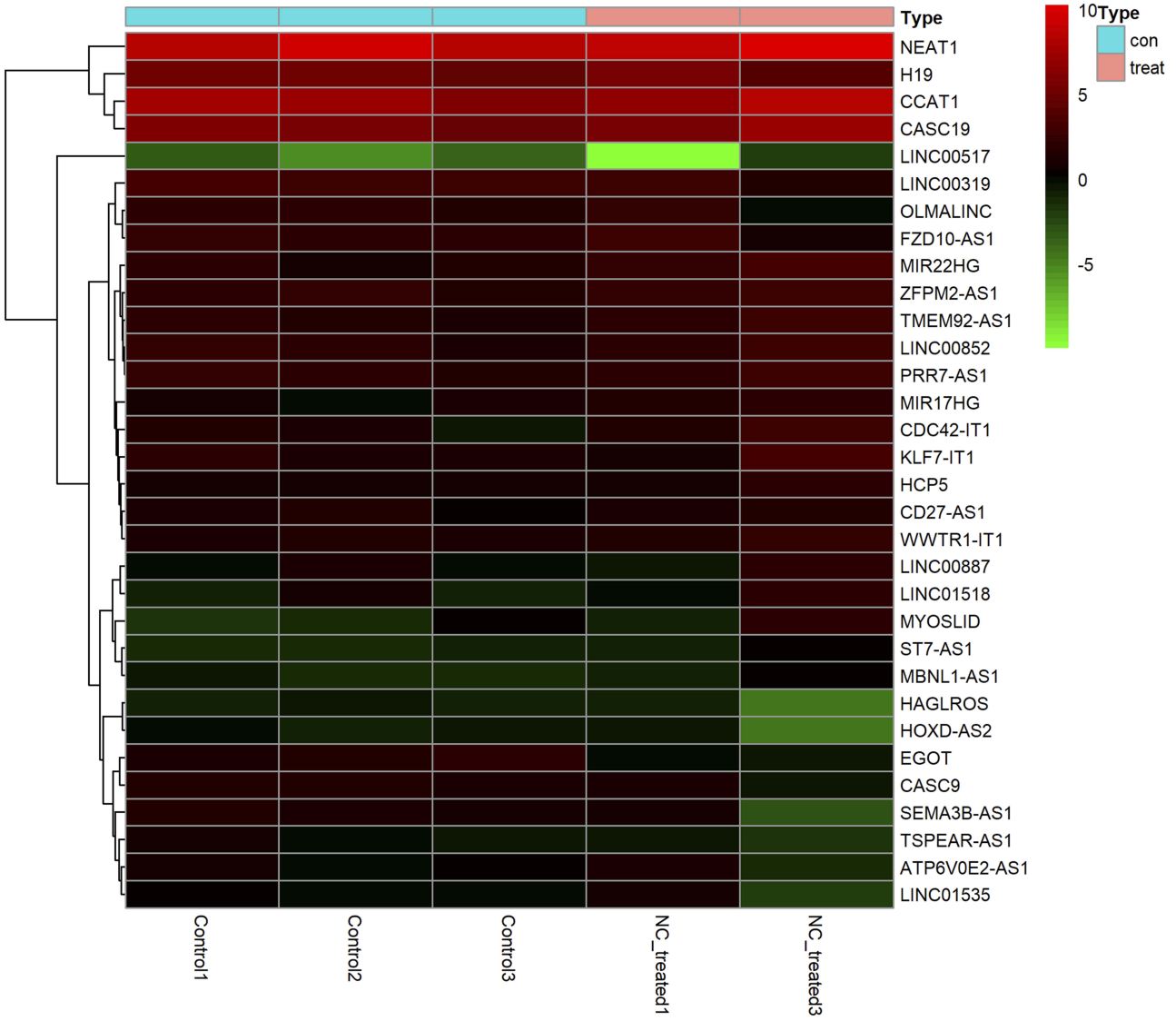

Figure 10 Heatmap of differentially expressed lncRNAs in nitidine chloride-treated hepatocellular carcinoma (HCC) xenografts The expression changes of differentially expressed lncRNAs between before and after nitidine chloride treatment in HCC xenografts are displayed in squares of colors ranging from green to red.

the miR-10a-5p/NCOR2 axis, HMGB1, or HuR to participate in the oncogenesis of HCC.[14,15] Our investigation of the molecular basis of *MIR22HG* in HCC also provided novel insights into the mechanism of *MIR22HG* in HCC. The finding of seven cases of deep deletion occurring in the TCGA provisional HCC samples from cBioPortal may explain the down-regulation of *MIR22HG* at the transcriptional level. The predicted *MIR22HG*-TF-mRNA triplets in HCC hinted that a binding reaction between *MIR22HG* and TFs, such as *CREBBP, POU2F2, ZZZ3, SIRT6*, and *EP300*, might participate in the initiation and development of HCC. Co-expression analysis for *MIR22HG* implicated the *MIR22HG*-related gene interaction network in HCC.

Several of the genes co-expressed with *MIR22HG*, including *NLRP3, CSF1R, SIGLEC10*, and *ZEB2*, were reported to play crucial roles in the initiation and progression of HCC.[28–31] Functional analysis of the co-expressed genes suggested a significant enrichment in molecular functions that included protein tyrosine kinase activity, non-membrane spanning protein tyrosine kinase activity, and phosphotyrosine residue binding, as well as activation of pathways involving hematopoietic cell lineage, viral protein interaction with cytokines and cytokine receptors, and activity of the Rap1 signaling

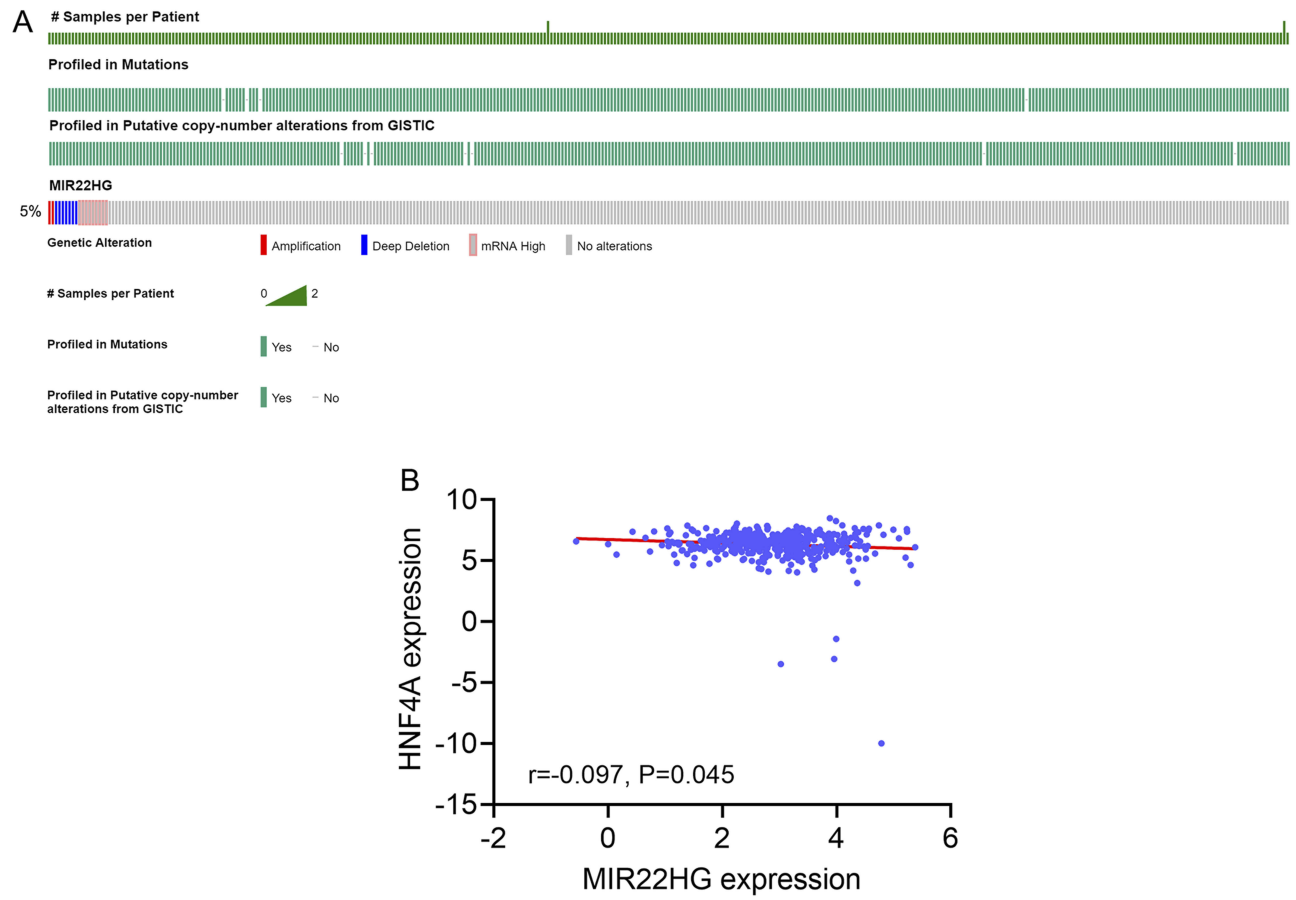

Figure 11 Gene alteration of *MIR22HG* in hepatocellular carcinoma (HCC) tissue and correlation between *MIR22HG* and one of the predicted transcription factors (**A**) Gene alteration of *MIR22HG* in HCC tissue from cBioPortal; (**B**) Correlation diagram of *MIR22HG* and HNF4A expression.

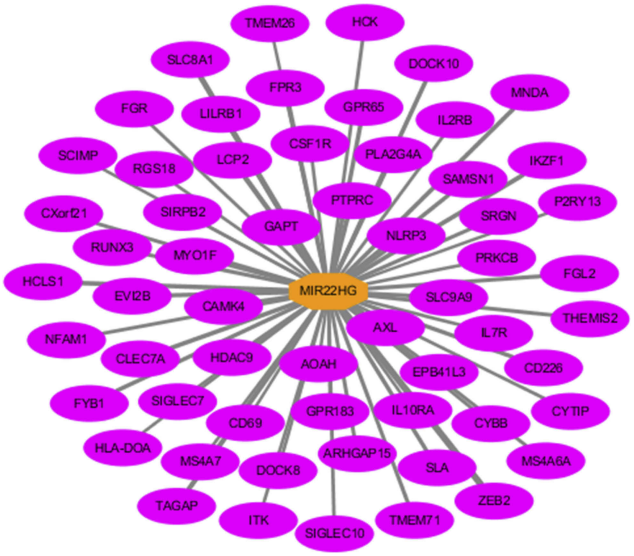

Figure 12 Co-expression network of *MIR22HG* in hepatocellular carcinoma (HCC) MIR22HG and its co-expressed genes are marked in red and yellow, respectively. The width of the links between genes represent the value of the weights.

pathway. We noted that the Rap1 signaling pathway was closely associated with the growth, invasion, and apoptosis of HCC cells. Mo et al reported that *EYA4* could attenuate the growth and invasion of HCC cells by repression of the NF-κB activity and *RAP1* expression.[32] In vitro experiments by Zha et al showed that knockdown of Rap1 led to 5-fluorouracil-induced apoptosis in HepG2 cells.[33] We postulated that the co-expressed genes may coordinate with *MIR22HG* to influence molecular functions and pathways essential for the oncogenesis of HCC, thereby affecting the development of HCC.

Unlike studies that investigated the mechanism of *MIR22HG* in HCC by focusing on the interplay between *MIR22HG* and specific miRNAs or mRNAs, our study has uncovered a new mechanism for *MIR22HG* in HCC using traditional Chinese medicine as the breakthrough point. Nitidine chloride is a natural alkaloid compound with proven anti-tumor effects in multiple human cancers, including osteosarcoma, ovarian cancer, acute myeloid leukemia, and HCC.[25,34–36] The impact of nitidine chloride on lncRNAs in cancer has never been studied previously,

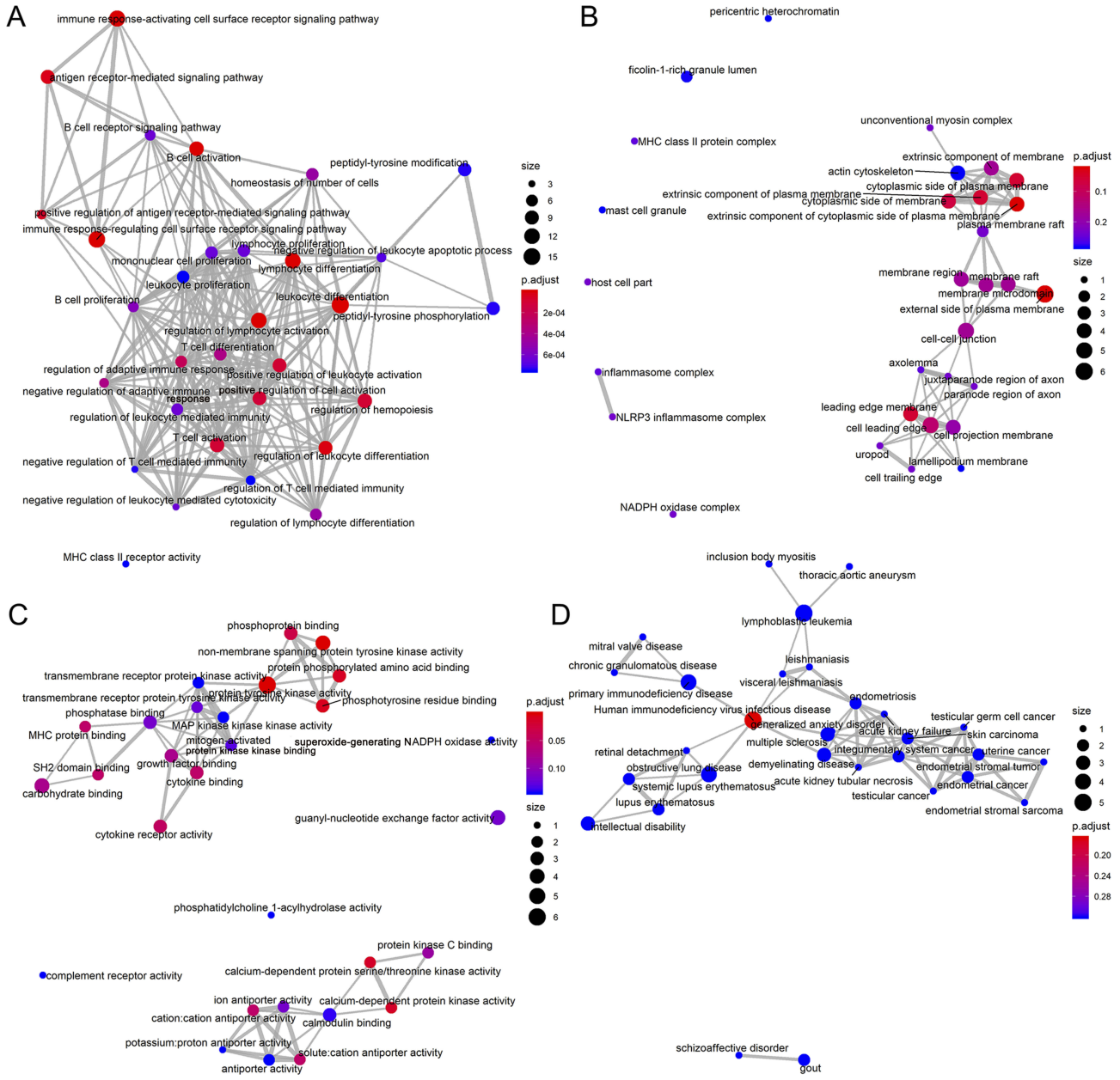

Figure 13 Gene ontology and disease ontology analysis for genes co-expressed with *MIR22HG* (**A**) Emapplot for significant terms of biological functions; (**B**) Emapplot for significant terms of cellular component; (**C**) Emapplot for significant terms of molecular functions; (**D**) Emapplot for significant terms of diseases.

so we conducted in vivo experiments to test whether nitidine chloride treatment might influence the expression of *MIR22HG* in HCC. The results demonstrated that nitidine chloride could stimulate *MIR22HG* expression in HCC xenografts, thereby implying that nitidine chloride and *MIR22HG* might have synergistic effects in the inhibition of HCC tumor growth.

The present study had several limitations that should be pointed out. The effect of *MIR22HG* on the function of HCC cells should be validated by in vitro or in vivo experiments. Limited by experiment support, expression of lncRNAs was sequenced in only three control and two NC-treated groups, which should be conducted with larger sample size. The interactions between *MIR22HG* and the predicted TFs, the co-expressed genes, and nitidine chloride also require further experiments. Further work is warranted to address these limitations.

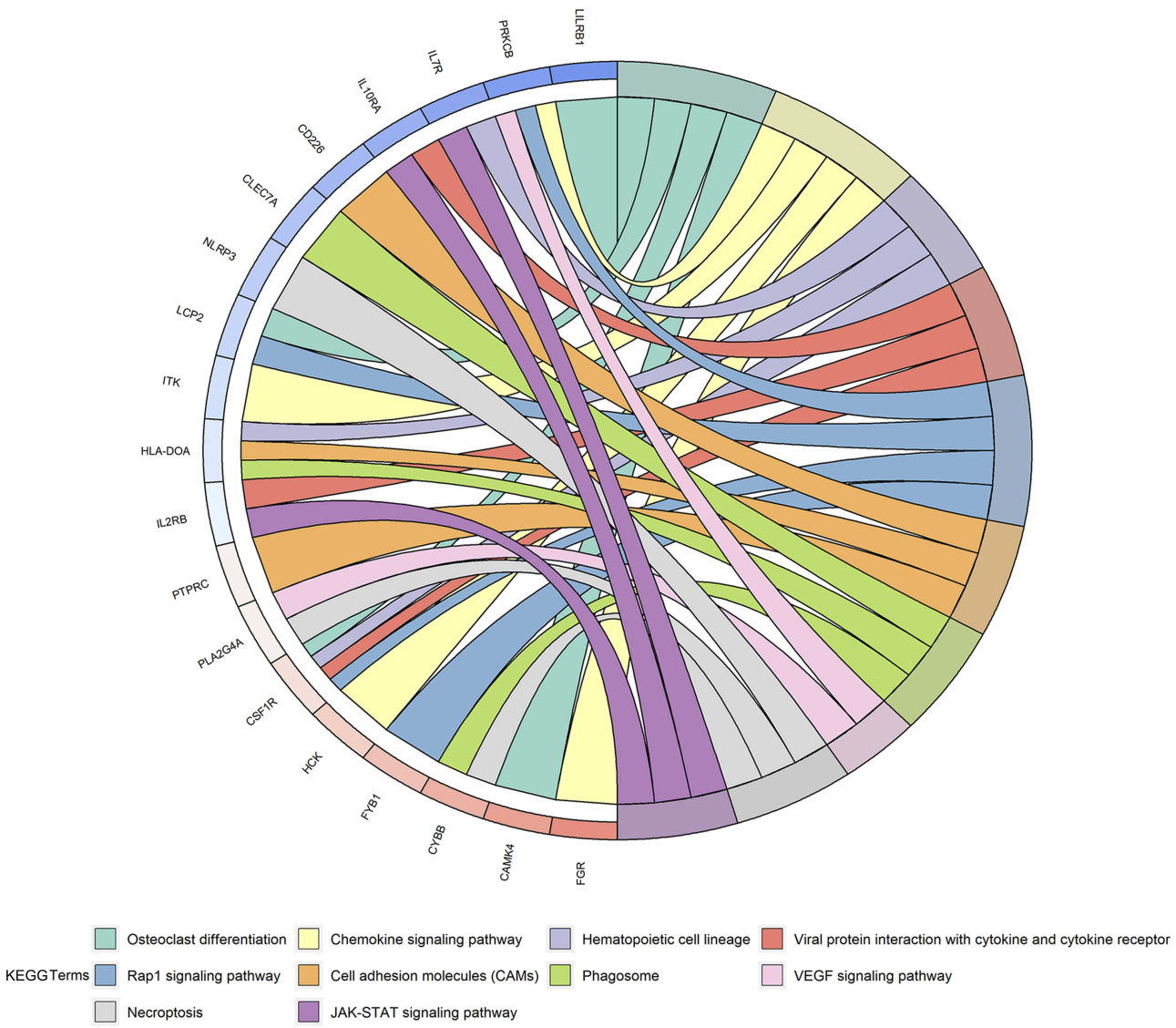

Figure 14 Kyoto encyclopedia of genes and genomes (KEGG) pathway analysis for co-expressed genes of *MIR22HG* Enrichment of co-expressed genes in significant KEGG pathway terms were visualized as a chord plot composed of ribbons.

Conclusion

In conclusion, we identified downregulation of *MIR22HG* and a protective effect of *MIR22HG* on the clinical progression and prognosis of HCC patients.

Ethics Approval And Informed Consent

All 101 patients with HCC provided signed informed consent and approval of this study was granted by the Ethics Committee of the First Affiliated Hospital of Guangxi Medical University. Approval for the use of nude mice in this study was granted by the Ethical Committee of First Affiliated Hospital of Guangxi Medical University (Nanning, Guangxi, China) (2018-KY-NSFC-102).

Data Availability

The datasets generated and/or analyzed during the current study are available in TCGA (https://portal.gdc.cancer.gov/), Arrayexpress (https://www.ebi.ac.uk/arrayexpress/), GEO (https://www.ncbi.nlm.nih.gov/gds/), cBioPortal (https://www.cbioportal.org/), and LncMAP (http://bio-bigdata.hrbmu.edu.cn/LncMAP/survival.jsp).

Acknowledgments

The authors would like to thank TCGA, Arrayexpress, GEO, cBioPortal and LncMAP databases for the availability of the data.

Funding

This study was supported by Fund of National Natural Science Foundation of China (NSFC 81860717, NSFC81560489), Fund of Natural Science Foundation of Guangxi, China (2018GXNSFAA294025, 2017GXNSFAA198017), Guangxi Degree and Postgraduate Education Reform and Development Research Projects of China (JGY2019050), Guangxi Medical University Training Program for Distinguished Young Scholars, Guangxi First-class Discipline Project for Pharmaceutical Sciences (No. GXFCDP-PS-2018), Medical Excellence Award Funded by the Creative Research Development Grant from the First Affiliated Hospital of Guangxi Medical University.

Disclosure

All authors declared no conflicts of interests in this work.

References

1. Fu J, Wang H. Precision diagnosis and treatment of liver cancer in China. *Cancer Lett*. 2018;412:283–288.
2. Zhao B, Lu Y, Cao X, et al. MiRNA-124 inhibits the proliferation, migration and invasion of cancer cell in hepatocellular carcinoma by downregulating lncRNA-UCA1. *Onco Targets Ther*. 2019;12:4509–4516.
3. Bertuccio P, Turati F, Carioli G, et al. Global trends and predictions in hepatocellular carcinoma mortality. *J Hepatol*. 2017;67:302–309.
4. Rich NE, Yopp AC, Singal AG. Medical management of hepatocellular carcinoma. *J Oncol Pract*. 2017;13:356–364.
5. Sun T, Liu H, Ming L. Multiple roles of autophagy in the sorafenib resistance of hepatocellular carcinoma. *Cell Physiol Biochem*. 2017;44:716–727.
6. Zhu YJ, Zheng B, Wang HY, et al. New knowledge of the mechanisms of sorafenib resistance in liver cancer. *Acta Pharmacol Sin*. 2017;38:614–622.
7. Tutusaus A, Stefanovic M, Boix L, et al. Antiapoptotic BCL-2 proteins determine sorafenib/regorafenib resistance and BH3-mimetic efficacy in hepatocellular carcinoma. *Oncotarget*. 2018;9:16701–16717.
8. Zhang Y, Liu J, Lv Y, et al. LncRNA meg3 suppresses hepatocellular carcinoma in vitro and vivo studies. *Am J Transl Res*. 2019;11:4089–4099.
9. Zeng Z, Xu FY, Zheng H, et al. LncRNA-MTA2TR functions as a promoter in pancreatic cancer via driving deacetylation-dependent accumulation of HIF-1alpha. *Theranostics*. 2019;9:5298–5314.
10. Zheng J, Zhang H, Ma R, et al. Long non-coding RNA KRT19P3 suppresses proliferation and metastasis through COPS7A-mediated NF-kappaB pathway in gastric cancer. *Oncogene*. Epub 2019 Aug 13.
11. Bhan A, Soleimani M, Mandal SS. Long Noncoding RNA and Cancer: A New Paradigm. *Cancer Res*. 2017;77:3965–3981.
12. Su W, Feng S, Chen X, et al. Silencing of long noncoding RNA MIR22HG triggers cell survival/death signaling via oncogenes YBX1, MET, and p21 in lung cancer. *Cancer Res*. 2018;78:3207–3219.
13. Cui Z, An X, Li J, et al. LncRNA MIR22HG negatively regulates miR-141-3p to enhance DAPK1 expression and inhibits endometrial carcinoma cells proliferation. *Biomed Pharmacother*. 2018;104:223–228.
14. Wu Y, Zhou Y, Huan L, et al. LncRNA MIR22HG inhibits growth, migration and invasion through regulating the miR-10a-5p/NCOR2 axis in hepatocellular carcinoma cells. *Cancer Sci*. 2019;110:973–984.
15. Zhang DY, Zou XJ, Cao CH, et al. Identification and functional characterization of long non-coding rna mir22hg as a tumor suppressor for hepatocellular carcinoma. *Theranostics*. 2018;8:3751–3765.
16. Dong Y, Yan W, Zhang SL, et al. Prognostic values of long non-coding RNA MIR22HG for patients with hepatocellular carcinoma after hepatectomy. *Oncotarget*. 2017;8:114041–114049.
17. Xiong DD, Li ZY, Liang L, et al. The LncRNA NEAT1 accelerates lung adenocarcinoma deterioration and binds to Mir-193a-3p as a competitive endogenous RNA. *Cell Physiol Biochem*. 2018;48:905–918.
18. Zhang Y, Huang JC, Cai KT, et al. Long noncoding RNA HOTTIP promotes hepatocellular carcinoma tumorigenesis and development: a comprehensive investigation based on bioinformatics, qRTPCR and metaanalysis of 393 cases. *Int J Oncol*. 2017;51:1705–1721.
19. Wen DY, Lin P, Pang YY, et al. Expression of the long intergenic non-protein coding RNA 665 (LINC00665) gene and the cell cycle in hepatocellular carcinoma using the cancer genome atlas, the gene expression omnibus, and quantitative real-time polymerase chain reaction. *Med Sci Monit*. 2018;24:2786–2808.
20. Gao J, Aksoy BA, Dogrusoz U, et al. Integrative analysis of complex cancer genomics and clinical profiles using the cBioPortal. *Sci Signal*. 2013;6:pl1.
21. Dang YW, Zeng J, He RQ, et al. Effects of miR-152 on cell growth inhibition, motility suppression and apoptosis induction in hepatocellular carcinoma cells. *Asian Pac J Cancer Prev*. 2014;15:4969–4976.
22. He RQ, Gao L, Ma J, et al. Oncogenic role of miR1835p in lung adenocarcinoma: a comprehensive study of qPCR, in vitro experiments and bioinformatic analysis. *Oncol Rep*. 2018;40:83–100.
23. Law CW, Chen Y, Shi W, et al. voom: precision weights unlock linear model analysis tools for RNA-seq read counts. *Genome Biol*. 2014;15:R29.
24. Liu LM, Lin P, Yang H, et al. Gene profiling of HepG2 cells following nitidine chloride treatment: an investigation with microarray and connectivity mapping. *Oncol Rep*. 2019;41:3244–3256.
25. Liu LM, Xiong DD, Lin P, et al. DNA topoisomerase 1 and 2A function as oncogenes in liver cancer and may be direct targets of nitidine chloride. *Int J Oncol*. 2018;53:1897–1912.
26. Wu Y, Wang PS, Wang BG, et al. Genomewide identification of a novel six-LncRNA signature to improve prognosis prediction in resectable hepatocellular carcinoma. *Cancer Med*. 2018;7:6219–6233.
27. Fu HX. Exploration the anti-angiogenesis effect of nitidine chloride based on mTOR signal pathway. *Guangxi Med Univ*. 2017;86.
28. Wei Q, Zhu R, Zhu J, et al. E2-induced activation of the NLRP3 inflammasome triggers pyroptosis and inhibits autophagy in HCC cells. *Oncol Res*. 2019;27:827–834.
29. Cai H, Zhu XD, Ao JY, et al. Colony-stimulating factor-1-induced AIF1 expression in tumor-associated macrophages enhances the progression of hepatocellular carcinoma. *Oncoimmunology*. 2017;6:e1333213.
30. Zhang P, Lu X, Tao K, et al. Siglec-10 is associated with survival and natural killer cell dysfunction in hepatocellular carcinoma. *J Surg Res*. 2015;194:107–113.
31. Gao HB, Gao FZ, Chen XF. MiRNA-1179 suppresses the metastasis of hepatocellular carcinoma by interacting with ZEB2. *Eur Rev Med Pharmacol Sci*. 2019;23:5149–5157.
32. Mo SJ, Hou X, Hao XY, et al. EYA4 inhibits hepatocellular carcinoma growth and invasion by suppressing NF-kappaB-dependent RAP1 transactivation. *Cancer Commun (Lond)*. 2018;38:9.

33. Zha Y, Gan P, Yao Q, et al. Downregulation of Rap1 promotes 5-fluorouracil-induced apoptosis in hepatocellular carcinoma cell line HepG2. *Oncol Rep*. 2014;31:1691–1698.
34. Xu H, Cao T, Zhang X, et al. Nitidine chloride inhibits SIN1 expression in osteosarcoma cells. *Mol Ther Oncolytics*. 2019;12:224–234.
35. Chen S, Yang L, Feng J. Nitidine chloride inhibits proliferation and induces apoptosis in ovarian cancer cells by activating the Fas signalling pathway. *J Pharm Pharmacol*. 2018;70:778–786.
36. Li P, Yan S, Dong X, et al. Cell cycle arrest and apoptosis induction activity of nitidine chloride on acute myeloid leukemia cells. *Med Chem*. 2018;14:60–66.